Tibetan plateau aridification linked to global cooling at the Eocene–Oligocene transition

Guillaume Dupont-Nivet[1], Wout Krijgsman[1], Cor G. Langereis[1], Hemmo A. Abels[2], Shuang Dai[3] & Xiaomin Fang[3,4]

Continental aridification and the intensification of the monsoons in Asia are generally attributed to uplift of the Tibetan plateau and to the land–sea redistributions associated with the continental collision of India and Asia[1–3], whereas some studies suggest that past changes in Asian environments are mainly governed by global climate[4–6]. The most dramatic climate event since the onset of the collision of India and Asia is the Eocene–Oligocene transition, an abrupt cooling step associated with the onset of glaciation in Antarctica 34 million years ago[7–9]. However, the influence of this global event on Asian environments is poorly understood. Here we use magnetostratigraphy and cyclostratigraphy to show that aridification, which is indicated by the disappearance of playa lake deposits in the northeastern Tibetan plateau, occurred precisely at the time of the Eocene–Oligocene transition. Our findings suggest that this global transition is linked to significant aridification and cooling in continental Asia recorded by palaeontological and palaeoenvironmental changes[10–12], and thus support the idea that global cooling is associated with the Eocene–Oligocene transition[13–15]. We show that, with sufficient age control on the sedimentary records, global climate can be distinguished from tectonism and recognized as a major contributor to continental Asian environments.

Global climate and regional tectonism affect palaeoenvironmental conditions that are recorded during the deposition and accumulation of sediments[16]. In Asia, climate models[1,3] have shown that uplift of the Tibetan plateau and retreat of the Paratethys epicontinental sea associated with the Indo-Asia collision during the Cenozoic era can result in monsoonal intensification, continental aridification and increased erosion. When recognized in the sedimentary records, these palaeoenvironmental conditions have thus been attributed to regional tectonism, although they can equally well indicate global climate changes[4–6]. The key to distinguishing climatic effects from those of tectonism is to date the regional expression of these processes in the geologic record with sufficient resolution and accuracy to enable correlation to global climatic events precisely calibrated in the marine realm. The exceptionally long (~30 million years, Myr) continuous sedimentary succession of the Xining basin[17] at the northeastern margin of the Tibetan plateau provides an excellent opportunity to study the sedimentary signature of tectonic and climatic processes during Eocene to Oligocene times. The stratigraphic sequence reveals a remarkably sharp and widespread change in depositional environment expressed regionally by the disappearance of massive gypsum layers. To determine the cause of this lithologic change, detailed lithofacies analyses and high-resolution dating were performed on two parallel sedimentary sections from the Xining basin (the Shuiwan and Xiejia sections; Fig. 1).

The lower part of the stratigraphy studied consists of regular alternations of laterally continuous gypsum layers and red mudstone beds

(Fig. 2). The red mudstone intervals consist of silty clay virtually devoid of sedimentary structures, suggesting alteration during extended sub-aerial exposure after sheet-flood events supplied the clastic mud. They are typical of a distal alluvial fan environment[16]. Gypsiferous intervals are decimetre- to metre-thick tabular, nodular or laminar beds of alabastrine massive gypsum showing some chickenwire structures and displacive enterolithic veins (Fig. 1). They can grade laterally into green mudstone with preserved lacustrine lamination and are indicative of various stages of chemical precipitation in a playa lake environment[16] (see Supplementary Table 1). The precipitation of evaporites in continental playa-type systems is
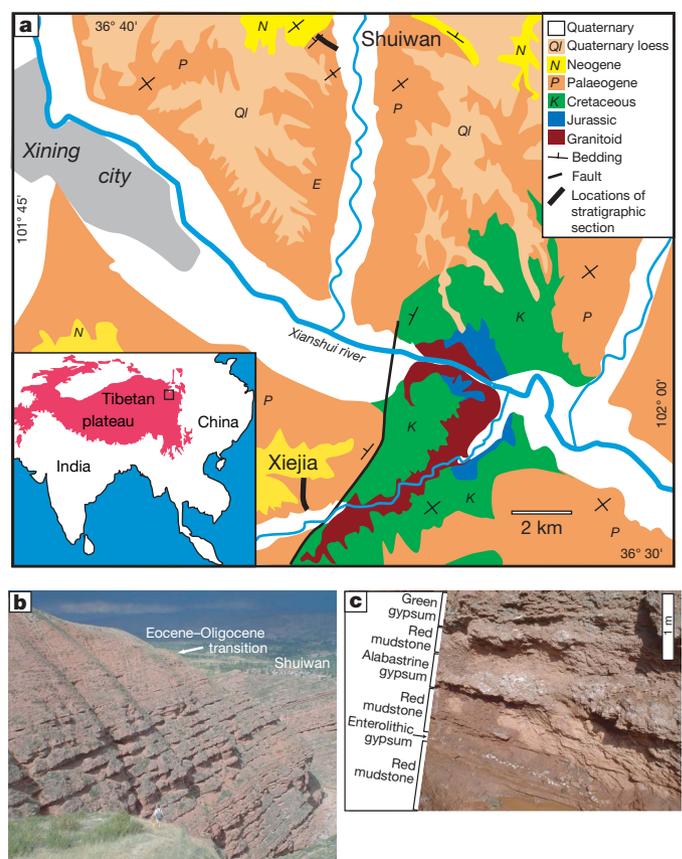

Figure 1 | Geologic setting. a, Location of studied stratigraphic sections. **b,** Field view to northeast, showing part of the Shuiwan section, including the end of cyclic gypsiferous deposition at the Eocene–Oligocene transition. **c,** Typical gypsum–mudstone cyclic alternations displaying characteristic lithofacies described in the text.

[1]Paleomagnetic Laboratory 'Fort Hoofddijk', Department of Earth Sciences, Utrecht University, Budapestlaan 17, [2]Stratigraphy-Paleontology, Department of Earth Sciences, Utrecht University, Budapestlaan 4, 3584 CD Utrecht, The Netherlands. [3]Lanzhou University, Key Laboratory of Western China's Environmental Systems, Gansu 730000, China. [4]Institute of Tibetan Plateau Research, Chinese Academy of Science, P O Box 2871, Beijing 100085, China.

chiefly determined by the supply of drained atmospheric water, ultimately providing solutes through groundwater inflow and overland runoff[18]. Gypsum intercalations within the red mudstones are thus indicative of periods with significantly higher water supply providing sufficient solutes to accumulate metre-scale gypsum layers[18]. The regularity of the gypsum/mudstone alternations indicate periodical fluctuations in atmospheric water supply to the basin, suggesting a cyclic mechanism most probably controlled by climate oscillations.

In the upper part of the stratigraphy, fully developed gypsum layers disappear. Sediments are dominated by homogenous red mudstones with minor interstitial gypsum content and occasional sandstone layers indicative of a distal alluvial fan depositional environment, without playa lake intercalations. The inhibition of gypsum accumulation between the lower and the upper part of the stratigraphy implies a permanent drop in the supply of atmospheric water that resulted in pronounced aridification of the Xining basin.

Consistent with this, regional palaeoenvironmental records also document aridification in the Eocene to Oligocene interval considered here. The fossil pollen records from the studied sediments of the Xining basin[19] indicate a drying and cooling environment, as indicated by an increase in herbs and conifers. North of the Tibetan plateau, an abrupt faunal turnover is linked to cooling and aridification, as indicated by the evolution of mammal tooth patterns and a drastic size decrease from large Eocene species (including some of the largest terrestrial mammals ever known) to small Oligocene species

dominated by rodents[10]. Moreover, the first extensive set of $\delta^{18}O$ and $\delta^{13}C$ isotopic data reveals a positive shift between Eocene and Oligocene continental strata that has been attributed to aridification[12].

To determine whether this aridification can be linked to tectonism or known climatic events in the Eocene to Oligocene interval, we accurately dated the sediments. Magnetostratigraphic sampling of the two sections was performed to determine the pattern of normal and reversed polarity intervals of the Earth's palaeomagnetic field. Palaeomagnetic analysis (see Methods and Supplementary Information) and the excellent consistency between the two records indicate a primary origin of the rock magnetization and the reliability of polarity intervals (Fig. 2). Our results improve and corroborate the long magnetostratigraphic records previously obtained from the Xining basin[17], showing a distinctive pattern of two long reversed intervals (R1 and R2) separated by a shorter normal interval (N2). This pattern provides a unique correlation to chrons C12r and C13r of the geomagnetic polarity timescale (GPTS[20]), which indicates that the sampled interval straddles the Eocene–Oligocene boundary, in agreement with palaeontological constraints[17,19] (see Methods). According to the GPTS correlation, the average period of gypsum–mudstone alternations is 109 thousand years (109 kyr) at Xiejia and 93 kyr at Shuiwan. These values are consistent with the ~100-kyr periodicity of the Earth's orbital eccentricity, suggesting that the supply of atmospheric water, periodically sufficient for gypsum
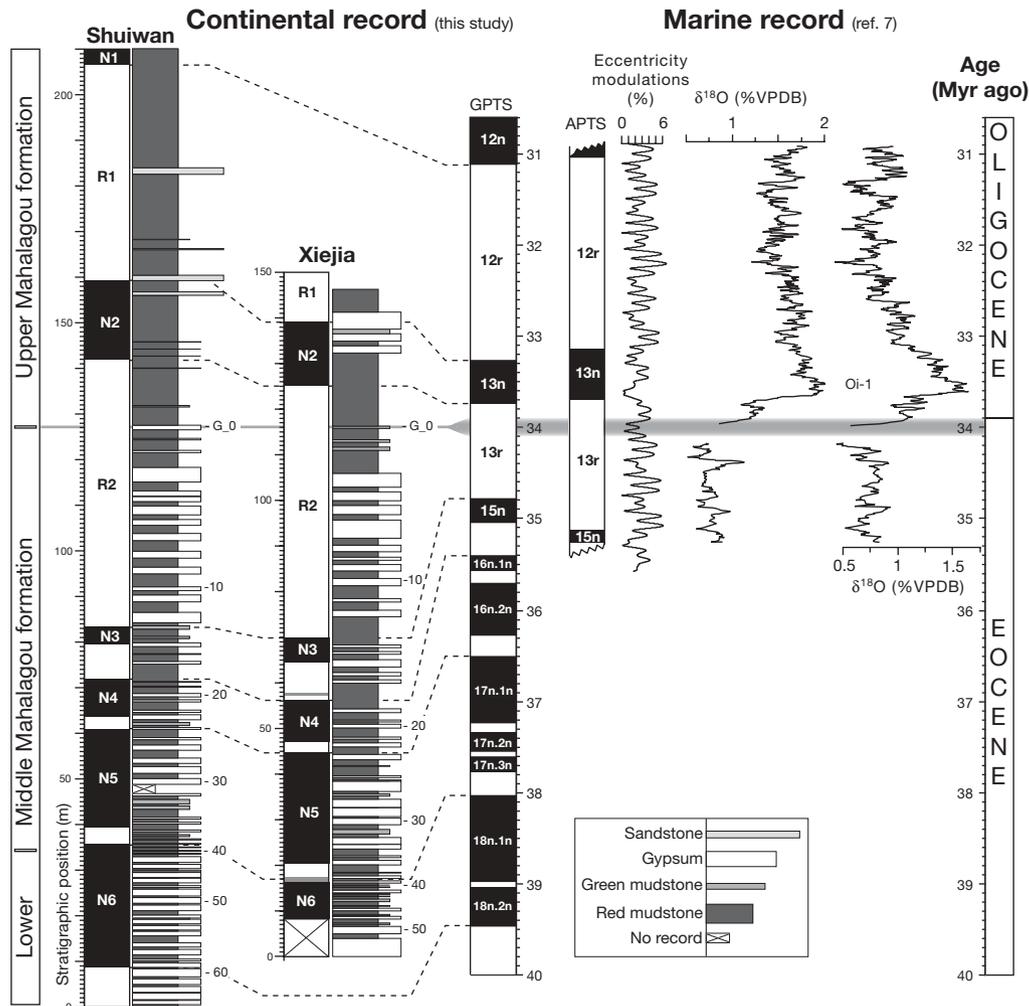

Figure 2 | Stratigraphic correlations. Lithostratigraphic descriptions are given in metres from the bottom of the Shuiwan and Xiejia sections. Eccentricity-driven gypsum–mudstone cycles are numbered down from the highest correlatable level G_0 at the lithofacies change. Observed normal (N)

and reverse (R) polarity zones (N1 to N6) are correlated to chrons of the GPTS[20] and the APTS[7]. Eccentricity modulation model is from ref. 22. The stable isotope shift is from the marine record at the Eocene–Oligocene transition[7]. VPDB, Vienna Pee-Dee Belemnite standard.

deposition, was controlled by eccentricity-driven climate variability. Pronounced aridification is defined by the interruption of this periodic system of basin-wide gypsum generation, above the highest gypsiferous level correlatable between the two sections (G_0 on Fig. 2). This layer marks the end of the distinctive pattern of regular gypsum–mudstone cycles, followed by mudstone-dominated successions with occasional non-correlative sandy and gypsiferous levels. In both sections, G_0 occurs near the top of C13r. Using linear interpolation between GPTS chron boundaries, G_0 is estimated at 34 Myr ago (33.9 Myr ago at Xiejia and 34.0 Myr ago at Shuiwan, Supplementary Table 4).

This age corresponds well with the most important step in Cenozoic global cooling 34 Myr ago, characterized by the onset of permanent Antarctic ice sheets at the Eocene–Oligocene transition and marked in the marine records by an abrupt increase in $\delta^{18}O$ and $\delta^{13}C$ values (the Oi-1 event)[7–9,21] (Fig. 2). This marine isotope increase was recently precisely documented as a two-step shift (40 kyr each) separated by an intermediate plateau (200 kyr)[7]. To formally compare our results with this marine record, we calibrate our data to the astronomically tuned polarity timescale (APTS) of this study[7], providing chron boundaries dated with respect to the variation of Earth's orbital parameters[22]. Linear interpolation between these chron boundaries also indicates a 34-Myr age for G_0 (33.9 at Xiejia and 34.1 at Shuiwan; Supplementary Table 4). Furthermore, the recognized eccentricity forcing of the gypsum–mudstone cyclicity enables us to test the consistency of our records directly with the astronomically tuned marine record. The number of eccentricity cycles expected to separate G_0 from the underlying chron C15n—according to the APTS—is indeed consistent at both sections with the number of observed gypsum–mudstone alternations separating G_0 from N3 (13 alternations at Shuiwan and Xiejia). This result independently validates our age estimate for G_0 at 34 Myr ago, indicating that the start of aridification after G_0 is coeval with the marine isotope shift of the climate transition (Fig. 2).

This remarkable correlation provides the first direct link between the Eocene–Oligocene climate transition and the aridification of continental Asia. In view of this finding, existing Eocene–Oligocene records of Asian environments must be interpreted with respect to climate change. The positive $\delta^{18}O$ and $\delta^{13}C$ shifts recorded north of the Tibetan plateau[12] can be attributed to the combined effects of aridification and the positive shift in isotopic values of ocean water (the ultimate source of meteoric water) at the Eocene–Oligocene transition. Abrupt changes in the Asian fauna in response to cooling and aridification (the Mongolian Remodelling)[10] can now be confidently linked to the Eocene–Oligocene transition and correlated to the large mammalian turnover in Europe (the 'Grande Coupure'), as well as globally reported continental and marine records of comparable faunal and floral turnovers at this time[13,21]. This supports the paradigm that the Eocene–Oligocene transition is associated with global atmospheric cooling and contrasts with recent claims, based on a few localized continental palaeotemperature estimates, that it may be linked to changes in Antarctic ice volume only[14,15]. Records of cooling and aridification[10–12,19] in the Asian interior are thus attributed to cooling of global ocean temperatures, reducing moisture supply to continental interiors. This effect may have been enhanced by a large Parathethys retreat induced by glacio-eustatic sea level lowering driven by Antarctic glaciation. Lastly, increasing sediment accumulation recorded over the East and Southeast Asian offshore region at about 33 Myr ago[23] now suggests that Eocene–Oligocene global cooling was also associated with increased regional erosion and sediment transport to the sea.

Our study demonstrates that global climate cooling must be recognized as a major contributor to Asian palaeoenvironment. It substantiates previous propositions that Pliocene climate deterioration or late Miocene global cooling essentially governed Asian depositional environments[4–6]. The growing evidence that global cooling is associated with continental aridification along with intensification of

monsoons and increased regional erosion remains to be tested by climate models. General circulation models have mainly focused on the effect of regional tectonism on Asian and global climate[1,3,24], showing that Tibetan uplift and Parathethys retreat can also increase Asian continental aridity, monsoons and erosion. Ultimately, Tibetan uplift can lead to global cooling through atmospheric circulation perturbations and carbon dioxide lowering associated with increased rock weathering[25].

Our results do not exclude that, in conjunction with the Eocene–Oligocene transition, tectonic processes have also contributed to Asian palaeoclimatic conditions. However, to establish the importance of these processes in driving Asian or global climate at this time, improved age control on their sedimentary expression is required. The Parathethys retreat is bracketed between late Eocene and latest Miocene time[26] and estimates for Tibetan plateau uplift range from the early Cenozoic at least 35 Myr ago[27,28] to the Pliocene 2–4 Myr ago[1]. In time, accurate and precise dating of Tibetan uplift may finally confirm the hypothesis that it was the primary cause of the Eocene–Oligocene climate transition through global atmospheric carbon dioxide lowering, instead of the recently challenged paradigm that the Eocene–Oligocene transition was triggered by the opening of a sea passage around Antartica[7–9,29]. Our study illustrates that distinguishing climate effects from tectonism can be accomplished by high-resolution dating, using magnetostratigraphy validated independently by the study of orbitally driven cyclicity in sediments[30]. This seems a promising tool for Asian sedimentary records, which often show cyclicity but are devoid of volcanics for radiometric calibration.

METHODS

Palaeomagnetic analysis. Palaeomagnetic sampling was performed in the course of two field seasons using a standard portable coring device; 187 and 110 sampling levels were collected in the 209.5-m-thick Shuiwan section and the 145.8-m-thick Xiejia section respectively (average sampling interval of 1.2 m). Palaeomagnetic analysis yielded reliable primary characteristic remanent magnetization directions at 206 levels (see Supplementary Figures 1 and 2 and Supplementary Tables 2 and 3). Polarity zones at the Shuiwan (12 zones) and Xiejia (10 zones) sections are defined by palaeomagnetic directions from three or more levels (Supplementary Fig. 3). Two questionable short polarity zones are defined by one sample only (depicted in grey on Fig. 2). Apart from these short intervals, the excellent consistency between the two magnetostratigraphic records strongly confirms the primary origin of the rock magnetization and the reliability of polarity intervals.

Palaeontological constraints. Palaeontological constraints provide a starting point for our age model (see palaeontological references in ref. 17). A relatively rich record of fossil mammals, ostracods, charophytes and pollen have been collected at the location of the two sampled sections (Xiejia and Shuiwan) including the Mahalagou formation (of interest for this study), the underlying Honggou formation, and the overlying Xiejia formation. The upper part of the Xiejia formation contains a well-documented mammal assemblage (the Xiejia fauna) that is described to be from the lowermost Miocene age (>20 Myr ago), implying that most of the Xiejia formation below this fossil locality is of Oligocene age. In addition, the lower part of the Xiejia formation is ascribed a late Oligocene age, the Mahalagou formation an early Oligocene age and the Honggou formation an Eocene age, on the basis of ostracods, charophytes and (mostly) pollen records[19]. Taken together, existing palaeontological constraints point to an early Oligocene age assignment for the sampled strata in the Mahalagou formation.

Magnetostratigraphic correlation. The complete pattern of magnetic polarity zones from the Honggou, Mahalagou and Xiejia formations recorded at the Xiejia and Shuiwan sections is provided by ref. 17. From this long record, two long reversed polarity zones separated by a shorter normal zone stand out clearly within the Mahalagou formation. Our focused palaeomagnetic sampling and analysis of this characteristic interval confirms this pattern and excludes the occurrences of the questionable short normal polarity intervals reported in the Xiejia section[17]. Above and below the pair of long reversed polarity zones are numerous shorter zones. When compared to the GPTS, the Early Oligocene to Late Eocene time interval is characterized by two long reversed chrons (C12r and C13r) separated by a shorter normal chron (C13n). Above and below this pair of long reversed chrons, the GPTS indicates shorter chrons. Given the palaeontological constraints and the pattern of magnetic polarity zones, the simplest

interpretation is to correlate the pair of long reversed polarity zones of the Mahalagou formation to the pair of reversed polarity chrons (C12r and C13r).

Although the shorter length of R1 relative to R2 is inverse to the pattern of C12r–C13r in the GPTS, alternative correlations of this pair of long reversed intervals are practically impossible. Correlating the long observed reversed intervals higher on the GPTS where the reversal rate is high would imply, at least, an order-of-magnitude increase in accumulation rates, fortuitously during the duration of these chrons. Correlation below would require these long reversed chrons to be expressed higher in the section, where recorded polarity zones are short, ultimately implying at least an order-of-magnitude decrease in accumulation rates. Such large variations would probably be indicated by facies variations (for example, conglomerates, disconformity or unconformity) that are not observed.

Below R2, we correlate N3 to C15n, N4 to C16n.1n–C16.2n, N5 to C17n.1n–C17n.2n–C17n.3n and N6 to C18n.1n–C18n.2n (Fig. 2). Supporting these correlations are the resulting consistent sedimentation rates calculated by linear interpolation between these chron boundaries (Supplementary Table 4). However, this correlation implies that four short reversed intervals have not been detected: C16n.1r = 159 kyr; C17n.1r = 131 kyr; C17n.2r = 72 kyr; and C18n.1r = 79 kyr. Given the low sedimentation rates, we argue that the following can explain the absence of these short intervals: (1) insufficient sampling resolution (average 1.2 m); (2) the absence of sampling in gypsum intervals yielding no palaeomagnetic signal; and (3) possible gaps in such sub-aerial deposits. An alternative in which no chrons are missed may be considered by correlating N5 to C16n.2n and N6 to C17n.1n. This alternative correlation would not change the magnetostratigraphic correlation of G_0 within C13r but we discarded it because the expected long normal interval C18n is not observed below N6 in the existing record[17], which shows instead a long reversed interval.

1. An, Z., Kutzbach, J. E., Prell, W. L. & Porter, S. C. Evolution of Asian monsoons and phased uplift of the Himalaya-Tibetan plateau since Late Miocene times. *Nature* **411**, 62–66 (2001).
2. Guo, Z. T. *et al.* Onset of Asian desertification by 22 Myr ago inferred from loess deposits in China. *Nature* **416**, 159–163 (2002).
3. Ramstein, G., Fluteau, F., Besse, J. & Joussaume, S. Effect of orogeny, plate motion and land–sea distribution on Eurasian climate change over the past 30 million years. *Nature* **386**, 788–795 (1997).
4. Gupta, A. K., Singh, R. K., Joseph, S. & Thomas, E. Indian Ocean high-productivity event (10–8 Ma): Linked to global cooling or to the initiation of the Indian monsoons? *Geology* **32**, 753–756 (2004).
5. Molnar, P. Late Cenozoic increase in accumulation rates of terrestrial sediments: How might climate change have affected erosion rates? *Annu. Rev. Earth Planet. Sci.* **32**, 67–89 (2004).
6. Zhang, P., Molnar, P. & Downs, W. Increased sedimentation rates and grain sizes 2–4 Myr ago due to the influence of climate change on erosion rates. *Nature* **410**, 891–897 (2001).
7. Coxall, H. K., Wilson, P. A., Palike, H., Lear, C. H. & Backman, J. Rapid stepwise onset of Antarctic glaciation and deeper calcite compensation in the Pacific Ocean. *Nature* **433**, 53–57 (2005).
8. DeConto, R. M. & Pollard, D. Rapid Cenozoic glaciation of Antarctica induced by declining atmospheric CO2. *Nature* **421**, 245–249 (2003).
9. Zachos, J. C. & Kump, L. R. Carbon cycle feedbacks and the initiation of Antarctic glaciation in the earliest Oligocene. *Glob. Planet. Change* **47**, 51–66 (2005).
10. Meng, J. & McKenna, M. C. Faunal turnovers of Palaeogene mammals from the Mongolian Plateau. *Nature* **394**, 364–367 (1998).
11. Garzione, C., Ikari, M. J. & Basu, A. R. Source of Oligocene to Pliocene sedimentary rocks in the Linxia basin in northeastern Tibet from Nd isotopes: Implications for

12. Graham, S. A. *et al.* Stable isotope records of Cenozoic climate and topography, Tibetan plateau and Tarim basin. *Am. J. Sci.* **305**, 101–118 (2005).
13. Ivany, L. C., Patterson, W. P. & Kyger, C. L. Cooler winters as a possible cause of mass extinctions at the Eocene/Oligocene boundary. *Nature* **407**, 887–890 (2000).
14. Grimes, S. T., Hooker, J. J., Collinson, M. E. & Mattey, D. P. Summer temperatures of late Eocene to early Oligocene freshwaters. *Geology* **33**, 189–192 (2005).
15. Kohn, M. J. *et al.* Climate stability across the Eocene-Oligocene transition, southern Argentina. *Geology* **32**, 621–624 (2004).
16. Talbot, M. R. & Allen, P. A. in *Sedimentary Environments: Processes, Facies and Stratigraphy* (ed. Reading, H. G.) 83–124 (Blackwell Publishing Inc., Oxford, 1996).
17. Dai, S. *et al.* Magnetostratigraphy of Cenozoic sediments from the Xining Basin: Tectonic implications for the northeastern Tibetan Plateau. *J. Geophys. Res.* **111**, doi:10.129/2005JB004187 (2006).
18. Yechieli, Y. & Wood, W. W. Hydrogeologic processes in saline systems: playas, sabkhas and saline lakes. *Earth Sci. Rev.* **58**, 343–365 (2002).
19. Wang, D.-N., Sun, X.-Y. & Zhao, Y.-N. Late Cretaceous to Tertiary palynofloras in Xinjiang and Qinghai, China. *Rev. Palaeobot. Palynol.* **65**, 95–104 (1990).
20. Ogg, J. G. & Smith, A. G. in *A Geologic Time Scale 2004* (eds Gradstein, F. M., Ogg, J. G. & Smith, A. G.) 63–86 (Cambridge Univ. Press, Cambridge, UK, 2004).
21. Prothero, D. R. in *Encyclopedia of Geology* (eds Selley, R., Cocks, R. & Plimer, I.) 472–478 (Elsevier, London, 2004).
22. Laskar, J. *et al.* A long-term numerical solution for the insolation quantities of the Earth. *Astron. Astrophys.*, doi:10.1051/0004–6361:20041335 (2004).
23. Clift, P. D., Layne, G. D. & Blusztajn, J. Marine sedimentary evidence for monsoon strengthening, Tibetan uplift and drainage evolution in Asia. Continent-ocean interactions in the East Asian marginal seas. *AGU Monogr.* **149**, 255–282 (2004).
24. Kutzbach, J. E. & Behling, P. Comparison of simulated changes of climate in Asia for two scenarios: Early Miocene to present, and present to future enhanced greenhouse. *Glob. Planet. Change* **41**, 157–165 (2004).
25. Ruddiman, W. F., Kutzbach, J. E. & Prentice, I. C. in *Tectonic Uplift and Climate Change* (ed. Ruddiman, W. F.) 203–235 (Plenum, New York, 1997).
26. Popov, S. *et al.* Lithological-paleogeographic maps of Paratethys 10 maps Late Eocene to Pliocene. *Courier Forschungsinstitut Senckenberg* **250**, 1–42 (2004).
27. Rowley, D. B. & Currie, B. S. Palaeo-altimetry of the late Eocene to Miocene Lunpola basin, central Tibet. *Nature* **439**, 677–681 (2006).
28. Harris, N. B. W. The elevation history of the Tibetan Plateau and its implications for the Asian monsoon. *Palaeogeogr. Palaeoclimatol. Palaeoecol.* **241**, 4–15 (2006).
29. Huber, M. *et al.* Eocene circulation of the Southern Ocean: Was Antarctica kept warm by subtropical waters? *Paleoceanography* **19**, doi:10.1029/2004PA001014 (2004).
30. Krijgsman, W. *et al.* Revised astrochronology for the Ain el Beida section (Atlantic Morocco): No glacio-eustatic control for the onset of the Messinian Salinity Crisis. *Stratigraphy* **1**, 87–101 (2004).